

**Heavy Higgs decay to  $t\bar{t}Z$  and constraints on a 750 GeV pseudoscalar**Bob Holdom<sup>\*</sup> and Melissa Ratzlaff<sup>†</sup>*Department of Physics, University of Toronto, Toronto, Ontario M5S1A7, Canada*

(Received 5 June 2016; published 18 July 2016)

In models with multiple nondegenerate Higgs bosons, the decay chain  $H/A \rightarrow A/HZ \rightarrow t\bar{t}Z$  may have a partial width comparable to the  $t\bar{t}$  decay mode. We recast the ATLAS standard model  $t\bar{t}Z$  measurement to put limits on the rate for this process. Limits are also set on the two Higgs doublet model at low  $\tan\beta$  that are sensitive to a heavy Higgs mass as high as  $\sim 750$  GeV. We then discuss the 750 GeV diphoton excess in terms of a pseudoscalar that also has the decays  $A \rightarrow HZ$  and  $A \rightarrow H^\pm W^\mp$ . These decays strongly constrain the partial widths for  $A \rightarrow \gamma\gamma$  and  $A \rightarrow gg$  when combined with the  $t\bar{t}$  resonance search limits. In a benchmark model the mass of  $H$  should be close to 650 GeV.

DOI: 10.1103/PhysRevD.94.015020

**I. HEAVY HIGGS TO  $t\bar{t}Z$** 

Some of the most popular extensions of the standard model (SM) include additional Higgs bosons. When sufficiently heavy a neutral Higgs boson ( $H$ ) and a pseudoscalar Higgs boson ( $A$ ) may have a dominant  $H/A \rightarrow t\bar{t}$  final state. The masses of the  $A$  and  $H$  need not be degenerate, and given a sufficient mass difference, the  $H/A \rightarrow A/HZ$  decay may compete with the  $H/A \rightarrow t\bar{t}$  decay. When the lighter Higgs boson ( $A$  or  $H$ ) is above the  $t\bar{t}$  threshold then it can be expected to have a dominant decay to  $t\bar{t}$ , leading to the final state  $t\bar{t}Z$ . This final state has a much smaller background than  $t\bar{t}$ . Also the  $HAZ$  coupling depends only on the gauge coupling times a factor that is unity in the alignment limit of the two Higgs doublet model (2HDM). Here we determine the first limits on the Higgs cascade decay to the  $t\bar{t}Z$  final state from the 8 TeV data. In the case that the lighter of  $A$  or  $H$  is below the  $t\bar{t}$  threshold, the limits from the resulting cascade decay to  $b\bar{b}Z$  have been considered in [1–4].

First we calculate the model independent limits on the  $H/A \rightarrow t\bar{t}Z$  process from the ATLAS  $t\bar{t}Z$  cross section measurement [5]. Second we use this process to constrain the masses in the 2HDM in the alignment limit. Finally we consider the implications from the  $A \rightarrow t\bar{t}Z$  and  $A \rightarrow H^\pm W^\mp$  decay modes when the pseudoscalar is consistent with the 750 GeV diphoton excess reported by ATLAS [6,7] and CMS [8,9].

**A. Model independent limits**

Both ATLAS [5] and CMS [10,11] have multilepton searches which measure the SM  $t\bar{t}Z$  production cross section at 8 TeV and also at 13 TeV [12,13]. Neither experiment sees a significant deviation from their SM expectations. The total theoretical SM  $t\bar{t}Z$  cross section

is  $\sim 200$  fb at  $\sqrt{s} = 8$  TeV. Due to the small size of this cross section, the 8 TeV data should provide useful limits on the process  $H/A \rightarrow A/HZ \rightarrow t\bar{t}Z$ . The strongest limit is given by a particular region of the ATLAS [5] search that has the following selection criteria:

- (i) four anti- $k_T$  jets with  $p_T > 25$  GeV,
- (ii) three leptons with  $p_T > 15$  GeV,
- (iii) on  $Z$  selection within 10 GeV of the  $Z$  mass,
- (iv) one  $b$  tagged jet.

We use CHECKMATE [14] to recast this signal region. We also include the jet-lepton overlap removal and an approximation to the lepton isolation criteria. We then validated our CHECKMATE analysis against a sample of SM  $t\bar{t}Z$  events generated with MADGRAPH [15] and showered with PYTHIA 6 [16]. We use a modified 2HDM FEYNRULES model [17] with HERWIG++ [18] to generate our signal events.

For the  $H$  production cross section we use the SM heavy Higgs gluon-gluon fusion cross section  $\sigma_{\text{SM}}$  from [19]. The  $A$  production cross section  $\sigma_{\text{SM}}^A$  is larger than  $\sigma_{\text{SM}}$  by a mass dependent scale factor that we deduce from the results in [20]. In Fig. 1 we show our resulting upper limits on the product of the branching ratios  $\text{Br}(H/A \rightarrow A/HZ)$  and  $\text{Br}(A/H \rightarrow t\bar{t})$  as a function of  $m_A$  and  $m_H$ . These results can easily be scaled to account for different values of the production cross sections.

Our signal has similar characteristics to the SM  $t\bar{t}Z$  production and if anything our signal has a higher acceptance times efficiency. Thus we can compare our signal with the  $t\bar{t}Z$  background for any given search and quickly estimate additional possible limits. We have not found more stringent limits from other available LHC searches.

**B. 2HDM limits in the alignment limit**

The 2HDM is a useful benchmark model in which to discuss these decays. In order to ensure that our results are consistent with a SM Higgs boson we work in the alignment limit where  $\sin(\beta - \alpha) = 1$ , and we set  $\lambda_6 = \lambda_7 = 0$  [21] as well. At tree level the  $H/A \rightarrow A/HZ$  decay is

<sup>\*</sup>bob.holdom@utoronto.ca  
<sup>†</sup>melissa.ratzlaff@gmail.com

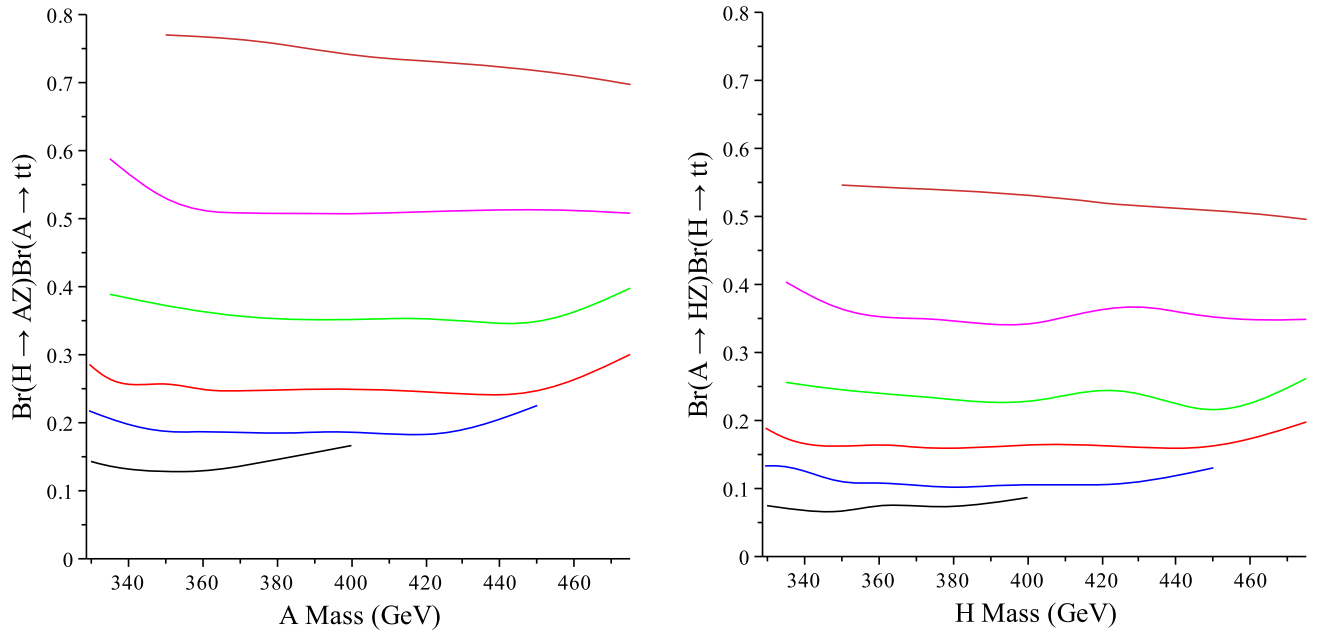


FIG. 1. The upper limits on  $\text{Br}(H \rightarrow AZ)\text{Br}(A \rightarrow t\bar{t})$  (left) and  $\text{Br}(A \rightarrow HZ)\text{Br}(H \rightarrow t\bar{t})$  (right) as a function of  $m_A$  ( $m_H$ ) (left and right, respectively). The masses of the heavier of  $A/H$  are from bottom to top 500 (black), 550 (blue), 600 (red), 650 (green), 700 (magenta), and 750 (orange) GeV.

proportional to  $\sin(\beta - \alpha)$  while the decays  $H \rightarrow WW$ ,  $ZZ$  and  $A \rightarrow hZ$  are proportional to  $\cos(\beta - \alpha)$  and are thus absent in the alignment limit. The  $H/A f\bar{f}$  couplings do not vanish in this limit and  $t\bar{t}$  becomes an important decay mode when  $m_{H/A} \gtrsim 2m_t$ . As long as this decay dominates

the other fermion decays our results are not very dependent on the type of the 2HDM. We use two Higgs doublet model calculator [22] to calculate the branching ratios for different values of  $m_H$  and  $m_A$ . We satisfy constraints from stability of the potential, unitarity and oblique parameters, in

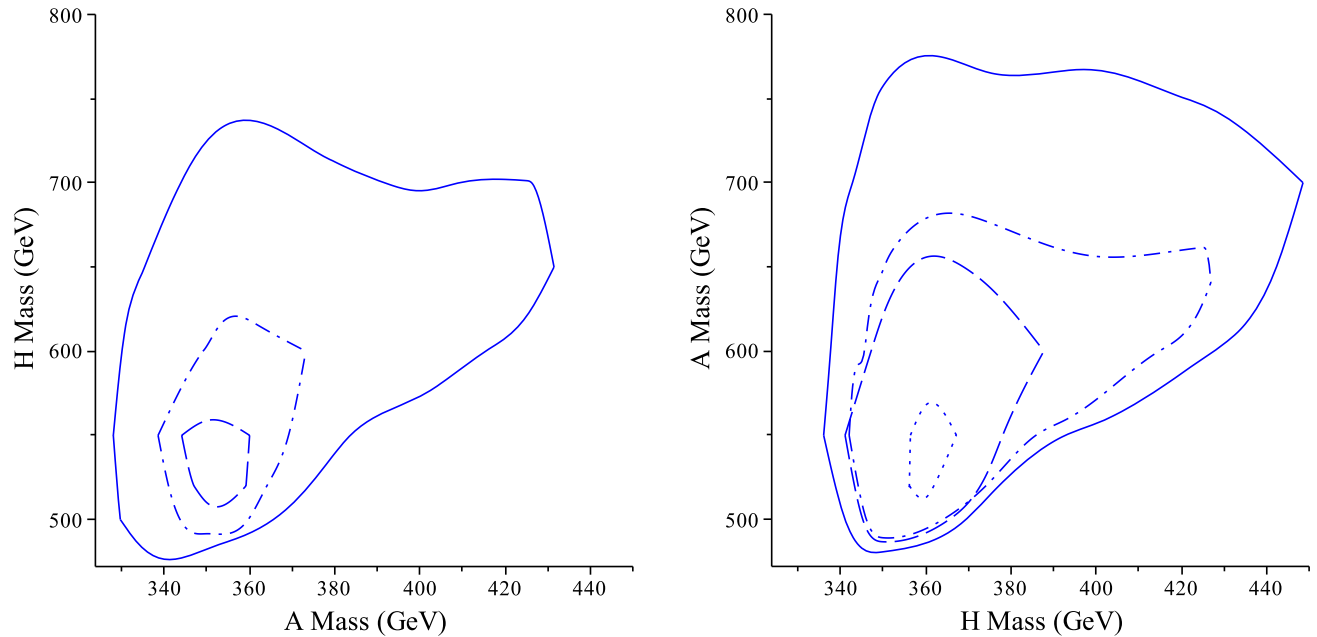


FIG. 2. The left (right) plot shows the mass limits for  $H \rightarrow AZ$  ( $A \rightarrow HZ$ ). The excluded region is enclosed by the solid curves for  $\tan\beta = 1$ , the dot-dashed curves for  $\tan\beta = 1.5$ , and the dotted curve for  $\tan\beta = 2$  (only in the  $A \rightarrow HZ$  case). The dashed curves are the limits when  $m_{H^\pm}$  is the lighter of  $A/H$  with  $\tan\beta = 1$ .

particular, by allowing  $m_{12}^2$  to be freely varying. Perturbativity is satisfied for most of the mass pairs.

We consider both of the cases  $m_H > m_A$  and  $m_A > m_H$  for some low values of  $\tan\beta$ . We set the charged Higgs mass to be the same as either the heavier or the lighter of  $H$  and  $A$ . In the latter case there is only a limit at  $\tan\beta = 1$  since the competing decay mode  $H/A \rightarrow H^\pm W^\mp$  is available with a somewhat larger branching ratio. The excluded mass regions with  $\tan\beta = \{1, 1.5, 2\}$  are shown in Fig. 2. Constraints on the large mass are as high as  $\sim 750$  GeV while constraints on the mass differences are as small as  $\sim 130$  GeV.

For the  $H^\pm W^\mp$  decay mode we consider  $A/H \rightarrow H^\pm W^\mp \rightarrow tbW \rightarrow WWbb$ , which has a large background from SM  $t\bar{t}$  production. We choose masses that are allowed from Fig. 2,  $m_{H^\pm} = 350$  GeV and  $m_{H/A} = 650$  GeV. We then scan the relevant searches available in CHECKMATE. We find that the signal contributes at most a relatively small number of events to some of the signal regions in [23–26].

We may use the ATLAS  $t\bar{t}Z$  measurement at 13 TeV [12] to help estimate future 13 TeV limits. Assuming the future observations are consistent with the SM,  $10 \text{ fb}^{-1}$  of data will provide comparable limits to our 8 TeV analysis. The improvement from  $100 \text{ fb}^{-1}$  of data is such that the dashed and dotted curves on the corresponding plots would move out to roughly the location of the solid curves in Fig. 2. The solid curves would extend out as far as  $\sim 900$  and  $\sim 550$  GeV in the vertical and horizontal directions respectively. The constraints on the mass differences would be as small as  $\sim 110$  GeV.

During the LHC run 2 other types of searches will further constrain heavy Higgs masses. Heavy Higgs boson production in association with top quarks,  $t\bar{t}H/A$  and  $tWbH/A$ , with  $H/A \rightarrow t\bar{t}$  is another process of interest for the alignment limit at low  $\tan\beta$ . With  $100 \text{ fb}^{-1}$  of data at 13 TeV this process can rule out a heavy Higgs mass in the 500 to 700 GeV range at  $\tan\beta = 1$  (see e.g. [27]). This process does not yield a corresponding constraint from the 8 TeV data.

## II. THE 750 GEV DIPHOTON EXCESS FROM $A \rightarrow \gamma\gamma$

Recently ATLAS [6,7] and CMS [8,9] have observed an excess of events in the diphoton spectrum at 750 GeV. We consider a 2HDM-like scenario where the possible 750 GeV state is a pseudoscalar ( $A$ ) that can decay to  $HZ$  and  $H^\pm W^\mp$ . We again ignore the  $H \rightarrow hh$ ,  $WW$ ,  $ZZ$  and  $A \rightarrow hZ$  decay modes that are not present at tree level in the alignment limit. We assume that the 2HDM is supplemented by additional heavy states so that the  $A \rightarrow \gamma\gamma$  and  $gg \rightarrow A$  rates are sufficiently enhanced. Some choices that we make, such as setting  $m_H = m_{H^\pm}$ , are motivated by a benchmark model that we outline below. Within this set of

TABLE I. The partial widths for  $A \rightarrow HZ$  ( $\Gamma_{HZ}^A$ ) and  $A \rightarrow H^\pm W^\mp$  ( $\Gamma_{H^\pm W^\mp}^A$ ).

$m_H = m_{H^\pm}$ GeV	550	600	625	640	650
$\Gamma_{HZ}^A$ GeV	9.6	3.2	1.3	0.48	0.15
$\Gamma_{H^\pm W^\mp}^A$ GeV	21	7.7	3.5	1.8	0.9
Limit $\sigma_{t\bar{t}Z}$ fb	106	114	117	132.5	147

assumptions we consider constraints coming from our  $t\bar{t}Z$  analysis and the CMS  $t\bar{t}$  resonance limits [28]. We consider  $m_H \geq 550$  GeV and the  $A \rightarrow t\bar{t}$  partial width in the range  $\Gamma_{t\bar{t}}^A = 0\text{--}40$  GeV. The upper end of this range is the natural width in the 2HDM at  $\tan\beta = 1$ .

The partial widths to  $HZ$  and  $H^\pm W^\mp$  at the masses that we consider are shown in Table I, as are our limits on the cross section for the production and decay of  $A$  ending with  $t\bar{t}Z$ .

We supplement the limits from our  $t\bar{t}Z$  analysis by limits on the  $A \rightarrow t\bar{t}$  decay. The CMS 8 TeV search for  $t\bar{t}$  resonances [28] sets an upper limit of  $\sigma_{t\bar{t}} < 0.3$  pb on a narrow scalar resonance at 750 GeV. The corresponding ATLAS limit is  $\sigma_{t\bar{t}} < 0.7$  pb [29]. Neither ATLAS nor CMS has a search for a wide width scalar  $t\bar{t}$  resonance. CMS [28] has a constraint on wide  $t\bar{t}$  resonance due to a 750 GeV  $Z'$ , where  $\sigma_{Z'} < 512$  fb for a 10% width. This provides a rough estimate for the wide width scalar limit.

The  $\gamma\gamma$  cross section should be  $\sim 4\text{--}9$  fb [30] in order to account for observed excess at 13 TeV. The corresponding 8 TeV cross section is  $\sim 0.6\text{--}2$  fb. There is also an upper limit of  $\sim 1.3$  fb from the CMS 8 TeV data [31] while the ATLAS 8 TeV limit is weaker [32]. We use  $\sigma_{\gamma\gamma} \sim 0.9$  fb at 8 TeV to accommodate the CMS limit and the 13 TeV excess. This value corresponds to the narrow width best fit value of  $\sim 4$  fb at 13 TeV [30].

We express these constraints on the  $\gamma\gamma$ ,  $t\bar{t}$  and  $t\bar{t}Z$  cross sections in terms of the partial widths for  $A \rightarrow gg$  ( $\Gamma_{gg}^A$ ) and  $A \rightarrow \gamma\gamma$  ( $\Gamma_{\gamma\gamma}^A$ ). We have

$$\sigma_{\gamma\gamma} = \frac{\Gamma_{\gamma\gamma}^A}{\Gamma_{\text{tot}}} \sigma_{\text{prod}}^A = \frac{\Gamma_{\gamma\gamma}^A}{\Gamma_{\text{tot}}} \frac{\Gamma_{gg}^A}{\Gamma_{\text{SM}}^A} \sigma_{\text{SM}}^A, \quad (1)$$

$$\Gamma_{\text{tot}} = \Gamma_{t\bar{t}}^A + \Gamma_{HZ}^A + \Gamma_{H^\pm W^\mp}^A + \Gamma_{gg}^A + \Gamma_{\gamma\gamma}^A + \Gamma_{\text{other}}. \quad (2)$$

The largest contributions to  $\Gamma_{\text{other}}$  are from  $b\bar{b}$  and  $\tau\bar{\tau}$ . The production cross section  $\sigma_{\text{prod}}^A$  is enhanced due to the loop contributions of new particles as reflected in the value of  $\Gamma_{gg}^A$ .<sup>1</sup> The observed value of  $\sigma_{\gamma\gamma}$  determines contours of fixed  $\Gamma_{t\bar{t}}^A$  as a function of  $\Gamma_{gg}^A$  and  $\Gamma_{\gamma\gamma}^A$ . The basic effect of the

<sup>1</sup>The remaining ratio is  $\sigma_{\text{SM}}^A/\Gamma_{\text{SM}}^A \sim 5 \times 10^3 \text{ fb/GeV}$  where we have used the same cross section  $\sigma_{\text{SM}}^A$  as in the first section.

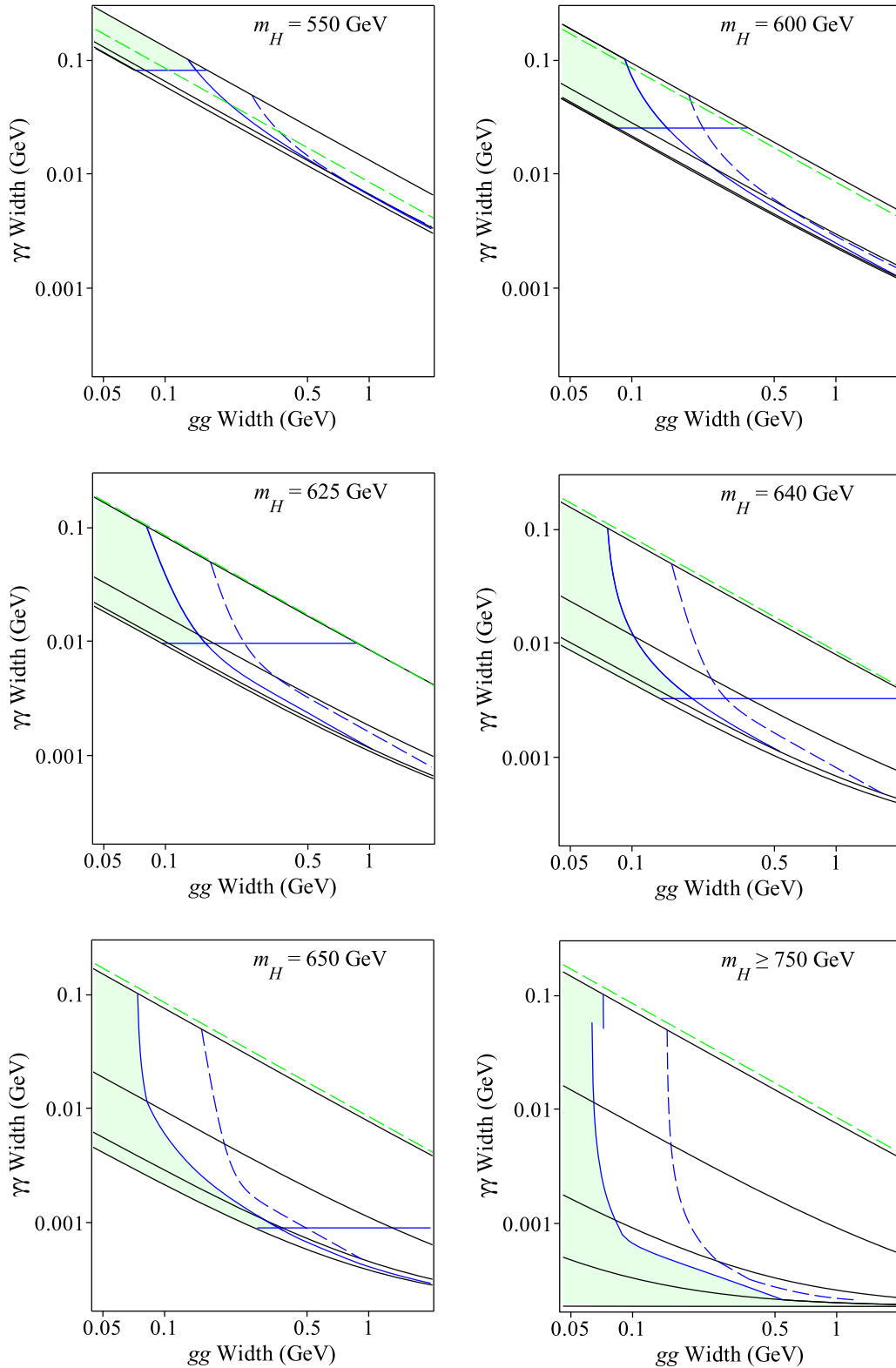


FIG. 3. The green shaded region shows the allowed values of the  $\gamma\gamma$  and  $gg$  widths consistent with  $\sigma_{\gamma\gamma} \sim 0.9$  fb at 8 TeV. The blue solid lines are the limits from  $t\bar{t}$  (curved line) and  $t\bar{t}Z$  (horizontal line). The dashed blue line is the ATLAS  $t\bar{t}$  limit. Fixed  $t\bar{t}$  widths correspond to the black curves where from bottom to top  $\Gamma_{t\bar{t}}^A \sim 0, 0.4, 4, 40$  GeV. The dashed green lines indicate a total width of  $\sim 45$  GeV. The  $m_H \gtrsim 750$  GeV case lacks a smooth continuation from the wide width to the narrow width limits, and for this case we have inserted an additional  $\Gamma_{t\bar{t}}^A \sim 0.08$  GeV curve.

TABLE II. The minimum (maximum) of the  $\gamma\gamma$  ( $gg$ ) partial width for various choices of  $\sigma_{\gamma\gamma}$  at 13 TeV. The corresponding value for the  $t\bar{t}$  partial width is also shown.

$m_H = m_{H^\pm}$ GeV	550	600	625	640	650
Max $\Gamma_{gg}^A$ GeV	0.14	0.15	0.16	0.185	0.36
$\Gamma_{t\bar{t}}^A$ GeV	32	8.3	3.3	1.3	0.31
Min $\Gamma_{\gamma\gamma}^A$ GeV at $\sigma_{\gamma\gamma} \sim 6$ fb	0.12	0.037	0.014	0.005	0.0013
Min $\Gamma_{\gamma\gamma}^A$ GeV at $\sigma_{\gamma\gamma} \sim 5$ fb	0.1	0.031	0.012	0.004	0.0011
Min $\Gamma_{\gamma\gamma}^A$ GeV at $\sigma_{\gamma\gamma} \sim 4$ fb	0.08	0.025	0.01	0.003	0.0009
Min $\Gamma_{\gamma\gamma}^A$ GeV at $\sigma_{\gamma\gamma} \sim 3$ fb	0.06	0.019	0.007	0.0024	0.00067

$HZ$  and  $H^\pm W^\mp$  decay modes is to push up the required value of the product  $\Gamma_{\gamma\gamma}^A \Gamma_{gg}^A$ .

The limits on the cross sections  $\sigma_{t\bar{t}}$  and  $\sigma_{t\bar{t}Z}$  can be written in terms of the partial widths as follows:

$$\sigma_{t\bar{t}} = \sigma_{\gamma\gamma} \frac{\Gamma_{t\bar{t}}^A}{\Gamma_{\gamma\gamma}^A}, \quad (3)$$

$$\sigma_{t\bar{t}Z} = \sigma_{\gamma\gamma} \frac{\Gamma_{HZ}^A \text{Br}(H \rightarrow t\bar{t})}{\Gamma_{\gamma\gamma}^A}. \quad (4)$$

The upper limits on  $\sigma_{t\bar{t}}$  and  $\sigma_{t\bar{t}Z}$  then determine the allowed regions on our plots. As can be seen from (4) and the results in Table I the  $t\bar{t}Z$  limit simply sets a  $m_H$  dependent minimum value for  $\Gamma_{\gamma\gamma}^A$ . [We expect that  $\text{Br}(H \rightarrow t\bar{t})$  is close to unity.] The allowed regions and the  $\Gamma_{t\bar{t}}^A$  contour curves are shown in Fig. 3.

The maximum allowed  $gg$  and the minimum allowed  $\gamma\gamma$  widths occur at the intersection point of the two limit curves in Fig. 3 and they are shown in Table II. Different possible choices of  $\sigma_{\gamma\gamma}$  at 13 TeV only affect the minimum  $\gamma\gamma$  widths as indicated in the table.

### A. Benchmark model

In order to provide some background for the choices we have made we briefly describe a benchmark model. Here the new heavy states are a chiral quark doublet  $\{t', b'\}$  and a chiral lepton doublet  $\{\tau', \nu'\}$  with SM charges. How such an extension of the SM is consistent with properties of the light Higgs boson is discussed in [33]. A four Higgs doublet model is thought to emerge as an effective description of the fluctuations around the chiral condensates of the four flavors  $t, t', b', \tau'$ . The lighter of these bosons have a flavor content dominated by  $t'$  and  $b'$  and they form a set that is 2HDM-like. For these states the  $H, H^\pm$  form an isotriplet and the  $A$  is an isosinglet relative to an approximate custodial symmetry in the  $t', b'$  sector. This implies that  $m_H \approx m_{H^\pm}$ . It also implies that while  $A$  has an enhanced production from gluon fusion,  $H$  has a suppressed production. We set  $m_{\nu'} = m_{b'} = 800$  GeV and choose  $m_{\tau'} > m_A/2$  to avoid the  $A \rightarrow \tau'\tau'$  decay. For the  $A$  widths of most interest to the  $\gamma\gamma$  signal we find

$\Gamma_{gg}^A \sim 0.25$  GeV and  $\Gamma_{\gamma\gamma}^A \sim 0.0015\text{--}0.004$  GeV, corresponding to  $m_{\nu'} = 700\text{--}775$  GeV.

From our results in Fig. 3 we see that  $m_H$  around 650 GeV can be consistent with these widths, namely the lower right corner of the allowed region in the  $m_H = 650$  GeV plot. But then in addition we see that the top width  $\Gamma_{t\bar{t}}^A$  needs to be reduced from its naive 2HDM value of  $\sim 40$  GeV. The  $A t\bar{t}$  coupling, along with other couplings of the bosons and their mass spectrum, is ultimately determined by the multi-Higgs potential. We find that parameters of this potential, partially already constrained by the light Higgs properties, can be constrained further such that  $\Gamma_{t\bar{t}}^A$  falls in the allowed range, e.g.  $\Gamma_{t\bar{t}}^A \lesssim 1$  GeV.<sup>2</sup> From the plot we also see how the  $t\bar{t}$  resonance searches of CMS and ATLAS differ on determining what this allowed range is. For larger  $m_H$ , the  $m_H \gtrsim 750$  GeV plot shows that the model parameters would have to be more tuned to obtain a sufficiently small  $\Gamma_{t\bar{t}}^A$ .

### B. $H^\pm W^\mp$ decays and leptonic decays

We turn now to the question of whether there can be direct limits due to the decay  $A \rightarrow H^\pm W^\mp$ . We consider the  $A \rightarrow Wtb$  decay and find an approximate upper limit from [24] using CHECKMATE. At  $m_{H^\pm} = 650$  GeV we estimate that the cross section limit is  $\sim 1$  pb for this final state, to be compared with the predicted value of  $\sigma_{H^\pm W^\mp}^A \sim 600$  fb when  $\text{Br}(H^\pm \rightarrow tb) = 1$ .<sup>3</sup> We note that if the width of the  $H^\pm$  is large (for example  $\sim 50$  GeV), the branching ratio to  $A \rightarrow H^\pm W^\mp$  where the  $H^\pm$  is virtual can remain quite unsuppressed beyond  $m_H > 660$  GeV. When this is the case then for such  $H$  masses the corresponding plot of the type in Fig. 3 can continue to look like the  $m_H = 650$  GeV plot (but without the limit from  $t\bar{t}Z$ ).

In the benchmark model another possible decay mode is  $H^\pm \rightarrow \tau'\nu'$ , and when kinematically open it can be a dominant decay mode that results in multilepton final states. We take the dominant heavy lepton decays to be

<sup>2</sup>The  $A\tau'\tau'$  coupling need not be so suppressed and it tends to enhance  $\Gamma_{\gamma\gamma}^A$ . The  $Ht\bar{t}$  coupling is suppressed, but still the  $t\bar{t}$  decay of  $H$  dominates.

<sup>3</sup>When  $m_{H^\pm} = m_H = 650$  GeV,  $\Gamma_{H^\pm W^\mp}^A \approx 6\Gamma_{HZ}^A$ .

$\tau' \rightarrow W\nu'$  (rather than  $\tau' \rightarrow W\nu_\tau$ ) and  $\nu' \rightarrow \tau W$  ( $\nu' \rightarrow \mu W$ ,  $eW$  would be even more striking). Then there is a quite striking final state,

$$A \rightarrow H^\pm W^\mp \rightarrow W\tau'\nu' \rightarrow WWW\tau\tau. \quad (5)$$

The cross section limits for this process from the ATLAS four or more lepton search [34] are approximately  $\lesssim 55\text{--}90$  fb when  $m_{\tau'} = 400$  GeV and  $m_{\nu'} = 100\text{--}200$  GeV. Given the size of  $\sigma_{H^\pm W^\mp}^A$  and any sizable  $H^\pm \rightarrow \tau'\nu'$  branching ratio, these data imply that the  $\nu'$  and  $\tau'$  masses are such that this cascade decay is either kinematically forbidden or at least kinematically suppressed.

### III. SUMMARY

When the masses of additional Higgs bosons are not degenerate, the  $A/H \rightarrow \tau\tau Z$  final state offers a relatively model independent and clean probe of the heavy Higgs sector. In the 2HDM (at low  $\tan\beta$  and close to the alignment limit) we found that it eliminates quite a large region of the  $m_H\text{--}m_A$  plane. In general any future search

that is sensitive to the  $\tau\tau Z$  standard model background may also be sensitive to this signal.

Assuming that a 750 GeV mass  $A$  is the source of the diphoton excess observed by ATLAS and CMS [6–9], we considered the impact of a lighter  $H$  that leads to the decay  $A \rightarrow HZ \rightarrow \tau\tau Z$ . Basically we find that the lighter the  $H$ , the larger the  $\gamma\gamma$  width of the  $A$  needs to be. In a benchmark model where the new fermions are  $t', b', \tau', \nu'$  and the  $\gamma\gamma$  width cannot be arbitrarily large, we find that  $m_H$  is constrained to a narrow range around 650 GeV. In this case the model predictions nearly saturate the bounds both from the  $\tau\tau Z$  SM search and the  $\tau\tau$  resonance search. The  $Wtb$  signal from the charged Higgs decay may also be of interest. Thus this picture should be quite testable as new LHC data emerge.

### ACKNOWLEDGMENT

This research was supported in part by the Natural Sciences and Engineering Research Council of Canada.

- 
- [1] B. Coleppa, F. Kling, and S. Su, *J. High Energy Phys.* **09** (2014) 161.
- [2] G. C. Dorsch, S. J. Huber, K. Mimasu, and J. M. No, *Phys. Rev. Lett.* **113**, 211802 (2014).
- [3] B. Holdom and M. Ratzlaff, *Phys. Rev. D* **91**, 035031 (2015).
- [4] G. C. Dorsch, S. J. Huber, K. Mimasu, and J. M. No, *Phys. Rev. D* **93**, 115033 (2016).
- [5] G. Aad *et al.* (ATLAS Collaboration), *J. High Energy Phys.* **11** (2015) 172.
- [6] The ATLAS Collaboration, Report No. ATLAS-CONF-2015-081.
- [7] The ATLAS Collaboration, Report No. ATLAS-CONF-2016-018.
- [8] The CMS Collaboration, Report No. CMS-PAS-EXO-15-004.
- [9] The CMS Collaboration, Report No. CMS-PAS-EXO-16-018.
- [10] V. Khachatryan *et al.* (CMS Collaboration), *Eur. Phys. J. C* **74**, 3060 (2014).
- [11] V. Khachatryan *et al.* (CMS Collaboration), *J. High Energy Phys.* **01** (2016) 096.
- [12] The ATLAS Collaboration, Report No. ATLAS-CONF-2016-003.
- [13] The CMS Collaboration, Report No. CMS-PAS-TOP-16-009.
- [14] M. Drees, H. Dreiner, D. Schmeier, J. Tattersall, and J. S. Kim, *Comput. Phys. Commun.* **187**, 227 (2015); J. de Favereau, C. Delaere, P. Demin, A. Giammanco, V. Lemaître, A. Mertens, and M. Selvaggi (DELPHES 3 Collaboration), *J. High Energy Phys.* **02** (2014) 057; M. Cacciari, G. P. Salam, and G. Soyez, *Eur. Phys. J. C* **72**, 1896 (2012); M. Cacciari and G. P. Salam, *Phys. Lett. B* **641**, 57 (2006); M. Cacciari, G. P. Salam, and G. Soyez, *J. High Energy Phys.* **04** (2008) 063; C. G. Lester and D. J. Summers, *Phys. Lett. B* **463**, 99 (1999); A. Barr, C. Lester, and P. Stephens, *J. Phys. G* **29**, 2343 (2003); Y. Bai, H. C. Cheng, J. Gallicchio, and J. Gu, *J. High Energy Phys.* **07** (2012) 110.
- [15] J. Alwall, R. Frederix, S. Frixione, V. Hirschi, F. Maltoni, O. Mattelaer, H.-S. Shao, T. Stelzer, P. Torrielli, and M. Zaro, *J. High Energy Phys.* **07** (2014) 079.
- [16] T. Sjostrand, S. Mrenna, and P. Z. Skands, *J. High Energy Phys.* **05** (2006) 026.
- [17] A. Alloul, N. D. Christensen, C. Degrande, C. Duhr, and B. Fuks, *Comput. Phys. Commun.* **185**, 2250 (2014).
- [18] M. Bahr, S. Gieseke, M. A. Gigg, D. Grellscheid, K. Hamilton, O. Latunde-Dada, S. Platzer, P. Richardson *et al.*, *Eur. Phys. J. C* **58**, 639 (2008).
- [19] S. Heinemeyer *et al.* (LHC Higgs Cross Section Working Group Collaboration), [arXiv:1307.1347](https://arxiv.org/abs/1307.1347).
- [20] J. F. Gunion, H. E. Haber, G. L. Kane, and S. Dawson, *The Higgs Hunter's Guide* (Brookhaven National Laboratory, New York, 1989), pp. 1–404 (2000).
- [21] J. F. Gunion and H. E. Haber, *Phys. Rev. D* **67**, 075019 (2003).
- [22] D. Eriksson, J. Rathsman, and O. Stal, *Comput. Phys. Commun.* **181**, 189 (2010).
- [23] G. Aad *et al.* (ATLAS Collaboration), *Eur. Phys. J. C* **74**, 2883 (2014).

- [24] G. Aad *et al.* (ATLAS Collaboration), *J. High Energy Phys.* **11** (2014) 118.
- [25] G. Aad *et al.* (ATLAS Collaboration), *Eur. Phys. J. C* **75**, 510 (2015).
- [26] The ATLAS Collaboration, Report No. ATLAS-CONF-2013-037.
- [27] N. Craig, J. Hajer, Y.Y. Li, T. Liu, and H. Zhang, [arXiv:1605.08744](https://arxiv.org/abs/1605.08744).
- [28] S. Chatrchyan *et al.* (CMS Collaboration), *Phys. Rev. Lett.* **111**, 211804 (2013); **112**, 119903 (2014).
- [29] G. Aad *et al.* (ATLAS Collaboration), *J. High Energy Phys.* **08** (2015) 148.
- [30] M. R. Buckley, *Eur. Phys. J. C* **76**, 345 (2016).
- [31] V. Khachatryan *et al.* (CMS Collaboration), *Phys. Lett. B* **750**, 494 (2015).
- [32] G. Aad *et al.* (ATLAS Collaboration), *Phys. Rev. D* **92**, 032004 (2015).
- [33] B. Holdom, *Phys. Rev. D* **90**, 015004 (2014).
- [34] The ATLAS Collaboration, Report No. ATLAS-CONF-2013-036.